An *in vitro* model of region-specific rib formation in chick axial skeleton: intercellular interaction between somite and lateral plate cells

Kaoru Matsutani[a], Koji Ikegami[a], Hirohiko Aoyama[a,b,*]

[a] Department of Anatomy and Developmental Biology, Graduate School of Biomedical Sciences, Hiroshima University, 1-2-3 Kasumi, Minami-ku, Hiroshima 734-8551, Japan.
[b] Present address; Department of Medical Science and Technology, Faculty of Health Sciences, Hiroshima International University, 555-36 Kurosegakuendai, Higashihiroshima city, Hiroshima 739-2695, Japan.

*Corresponding author
Department of Medical Science and Technology, Faculty of Health Sciences, Hiroshima International University, 555-36 Kurosegakuendai, Higashihiroshima city, Hiroshima 739-2695, Japan.; Email: aoyamah@hiroshima-u.ac.jp; Phone No: +81.823.70.4633; Fax No: +81.823.70.4542

Abstract

The axial skeleton is divided into different regions based on its morphological features. In particular, in birds and mammals, ribs are present only in the thoracic region. The axial skeleton is derived from a series of somites. In the thoracic region of the axial skeleton, descendants of somites coherently penetrate into the somatic mesoderm to form ribs. In regions other than the thoracic, descendants of somites do not penetrate the somatic lateral plate mesoderm. We performed live-cell time-lapse imaging to investigate the difference in the migration of a somite cell after contact with the somatic lateral plate mesoderm obtained from different regions of anterior–posterior axis *in vitro* on cytophilic narrow paths. We found that a thoracic somite cell continues to migrate after contact with the thoracic somatic lateral plate mesoderm, whereas it ceases migration after contact with the lumbar somatic lateral plate mesoderm. This suggests that cell–cell interaction works as an important guidance cue that regulates migration of somite cells. We surmise that the thoracic somatic lateral plate mesoderm exhibits region-specific competence to allow penetration of somite cells, whereas the lumbosacral somatic lateral plate mesoderm repels somite cells by contact inhibition of locomotion. The differences in the behavior of the somatic lateral plate mesoderm toward somite cells may confirm the distinction between different regions of the axial skeleton.

Keywords

Chick, Somite, Lateral plate, Intercellular interaction, Axial skeleton, Morphogenesis

1. Introduction

Cell migration is considered one of the fundamental processes in embryo morphogenesis (Le Douarin, 1984; Reig et al., 2014). Cell migration behavior can change by some signals, and depending on the source of the signal and the way it is received, signaling mechanisms are classified into chemotaxis, haptotaxis, contact guidance, contact inhibition of locomotion (CIL), and cell–cell adhesion (Jotereau and Le Douarin, 1982; Hernandez-Fleming et al., 2017; Carter, 1965; de la Loza et al., 2017; Laumonnerie et al., 2015; Kridsada et al., 2018; Abercrombie and Heaysman, 1954; Carmona-Fontaine et al., 2008; Villar-Cervino et al., 2013; Davis et al., 2015; Takeichi, 2014; Mayor and Etienne-Manneville, 2016; Scarpa and Mayor, 2016; Cousin, 2017). Migratory behavior of cells may be regulated by combinations of these guidance cues.

The axial skeleton of the trunk comprises a series of metamerically arranged vertebrae. The rib is such a characteristic thoracic structure that distinguishes the thorax from other regions of the axial skeleton in birds and mammals. The axial skeleton is derived from somites. Although thoracic somites have the potency to form ribs (Kieny et al., 1972), its exertion depends on the neighboring tissues around somites. In birds, a rib is composed of three compartments, viz., proximal rib, vertebro-distal rib, and sterno-distal rib, according to developmental dependencies of the adjacent tissues (Aoyama et al., 2005). The proximal rib is derived from a caudal half of somites under the influence of the ventral neural tube and notochord; the distal rib is derived from a caudal and rostral half of two adjacent somites (and ventrolateral lip of myotome or its periphery) under the influence of the surface ectoderm. Furthermore, the sterno-distal rib develops in relation to penetration into the somatic lateral plate mesoderm (LP) (Kato and Aoyama, 1998; Nowicki and Burke, 2000; Aoyama and Asamoto, 2000; Huang et al., 2000; Sudo et al., 2001; Aoyama et al., 2005).

It has been reported that interaction between thoracic somites and thoracic LP is important for the development of the sterno-distal rib. When the thoracic segmental plate is ectopically transplanted into the cervical region, the ribs derived from the explants are shorter than normal ribs (Kieny et al., 1972; Shearman and Burke, 2009). A blockage between thoracic somites and LP causes the absence of sterno-distal ribs

(Sudo et al., 2001). Liem and Aoyama (2009) reported that when LP of the limb-forming region is transplanted into the thoracic region, sterno-distal ribs are truncated or absent with an ectopically formed wing or leg (Liem and Aoyama, 2009). However, when the thoracic segmental plate is transplanted into the lumbosacral region, the grafted mesoderm forms ectopic ribs that have been much shorter than normal ribs (our unpublished data).

Here, we established an *in vitro* co-culture system to investigate somite cell behavior interacting with LP cells. We found that thoracic somite cells change their direction of migration after contact with lumbar LP (LP-lu) cells but not after contact with thoracic LP (LP-th) cells.

2. Results

2.1. Co-culture experiment on a two-dimensional (2D) substrate: behavior of thoracic somite cells on contact with LP-th or LP-lu cells

The isolated tissues were co-cultured in a liquid culture medium in a conventional glass base dish. The co-cultured tissues were as follows: thoracic somites (24th–25th somites) with LP-th (LP at 23rd–25th somite level) (Fig. 1A) and thoracic somites (21st–22nd somites) with LP-lu (LP at 30th–31st somite level) (Fig. 1B). Position of the nucleus in a time-lapse image was recorded every 10 min, and the direction of migration was evaluated. The direction of migration was compared between the tissues for 100 min before and after contact with a co-cultured cell (Fig. 1C and D).

We tested the null hypothesis that the direction of thoracic somite cell migration is unchanged before and after contact. The null hypothesis was rejected with two combinations, thoracic somites with LP-th and with LP-lu. There were significant differences between the direction of migration before and after contact (Fig. 1C and D). However, changes in the direction of migration were different among the co-culture combinations when comparing two components, i.e., a component leaving from the explant to the opposite explant and a component returning to the explant from the opposite explant, along a line between the explants. Before contact, 85.5% of thoracic somite cells migrated forward, and after contact with LP-th, 60.6% of somite cells migrated forward (Fig. 1C). However, before contact with LP-lu, 71.2% of thoracic

somite cells migrated forward, and after contact, 53.1% of somite cells migrated backward (Fig. 1D).

Quantitative analysis was difficult in this assay because the cells migrated in various directions with changing migration speed. Moreover, a cell may successively or simultaneously contact several cells.

Therefore, we performed another assay on a one-dimensional (1D) substrate wherein the cells migrated along narrow paths (Fig. 2A). This system allowed us to analyze the migratory behavior of a cell making contact with another cell in terms of only their speed.

2.2. Co-culture experiment on a 1D substrate: thoracic or lumbar somite derivatives with LP-th or LP-lu cells

We co-cultured the somite mesoderm with LP on CytoGraph in which the cytophilic area is restricted (10-μm wide paths) (Fig. 2A). The cells migrated away from the explants on the cytophilic paths and made contact with the cell migrating from the opposite side after 12–18 h (Fig. 2B and C). The cell had to migrate either forward or backward because it was confined to move on a cytophilic path. The velocity of a cell represents both the direction and speed of cell migration, i.e., positive and negative velocity values indicate that the cell migrated forward and backward, respectively. We observed various patterns of migration. For example, a cell continuously migrated forward by pushing aside other cells, a cell changed its direction of migration to backward, and a cell almost stopped migrating on contact. To determine the effect of intercellular interaction between somite and LP cells on contact, we tracked the points of leading and trailing edges of the cells (Fig. 2D) using consecutive images and calculated the migration velocity (μm/min). In Fig. 3, each line represents a cell whose leading and trailing edges (Fig. 2D) were tracked; the lines show migration 60 min before and after contact with co-cultured cells.

2.3. Behavior of thoracic sclerotome (SC-th) cells co-cultured with LP-th or LP-lu cells

Before contact, there was no significant difference in the migration velocity of SC-th and dermomyotome (DM) cells. When SC-th cells were co-cultured with LP-th or LP-lu cells, their average migrating velocity at the leading edge was 1.36 ± 0.23 μm/min (n = 11) and 1.56 ± 0.37 μm/min (n = 11), respectively (Fig. 4A). However, after contact with LP-th or LP-lu cells, the velocity decreased to 0.46 ± 0.15 μm/min (n = 11) and −0.55 ± 0.23 μm/min (n = 11), respectively, wherein the negative value represents backward migration (Fig. 4A). Although contact with LP-th cells decreased the velocity of SC-th cell migration by 34%, SC-th cell continuously migrated forward. However, contact with LP-lu cells altered SC-th cell movement to the opposite direction.

Cells on the CytoGraph did not necessarily migrate at a constant velocity, and the velocity varied from cell to cell. Figs. 4B and C show the relative frequency of cells (percentage) migrating at a certain velocity. Here, the velocity was represented as that of the leading edge. Velocity data were classified into eight classes at intervals of 1 μm/min (Fig. 4B and C). Bar graph on the right side represents forward movement and that on the left side represents backward movement.

Based on these data, we analyzed the migratory behavior of somite cells before and after contact with LP cells.

Most SC-th cells (66.7%) continuously migrated forward after contact with LP-th cells, although their speed became relatively low (Fig. 4B). Thirty minutes before contact, 24.1% SC-th cells migrated at the speed of 0–1 μm/min, whereas the percentage of cells increased to 48.5% after contact (Fig. 4B). In contrast, most SC-th cells (66.7%) migrated backward after contact with LP-lu cells (Fig. 4C). Moreover, more than 10% of the cells migrated backward at a velocity of more than 3 μm/min 30–60 min after contact (Fig. 4C). Thus, after contacting LP cells, the direction of migration of SC-th cells depended on the rostro-caudal level of LP cells.

2.4. Behavior of LP-th and LP-lu cells co-cultured with SC-th

Most LP-th cells migrated forward (88.7%) at a high speed (average velocity of 1.58 ± 0.39 μm/min; n = 11) before contact with SC-th cells (Fig. 4D and E). Figs. 4E and F show the proportions of cells migrating at different velocities. To calculate the velocity of a cell, the movement of its leading edge was measured. Velocity data were classified into eight classes, with intervals of 1 μm/min (Fig. 4E and F). Within 30 min after contact, although LP-th cells still predominantly migrated forward (60.6%; Fig. 4E), more than 30% of LP-th cells changed their direction of migration. This tendency was more conspicuous 30–60 min after contact. However, the velocity of LP-lu cells did not significantly change before and after contact with SC-th cells (Fig. 4D and F).

2.5. Behavior of thoracic DM (DM-th) cells co-cultured with LP-th and LP-lu cells

Most DM-th cells migrated forward 30 min before contact with LP-th cells (78.8%; average velocity of 1.02 ± 0.35 μm/min; n = 11), whereas most DM-th cells migrated in the opposite direction after contact (75.8%; average velocity of −0.56 ± 0.25 μm/min; n = 11) (Fig. 5A and B). We observed that LP-th cells with their leading edge in contact with the trailing edge of DM-th cells elongated backward in six of 11 cases (Fig. 3C). After contact with LP-th cells, DM-th cells exhibited stagnation in its leading edge and extension of the trailing edge, suggesting that these cells were to migrate backward but were unable to move due to cell–cell adhesion.

Within 30 min before contact with LP-lu cells, more than 70% of DM-th cells migrated forward (average velocity of 1.37 ± 0.40 μm/min; n = 11), whereas within 30 min after contact, approximately 50% of the cells migrated backward (average velocity of −0.59 ± 0.33 μm/min; n = 11) (Fig. 5A and C). In particular, more than 20% of cells migrated backward at a velocity of more than 2 μm/min. On contact with LP-lu cells, DM-th cells exhibited a sudden regression in the leading edge and backward extension of the trailing edge in five of 11 cases (Fig. 3D).

2.6. Behavior of LP-th and LP-lu cells co-cultured with DM-th cells

Before contact with DM-th cells, LP-th cells migrated forward at a high speed (average velocity of 1.91 ± 0.26 μm/min; n = 11), whereas their average velocity decreased significantly to 0.43 ± 0.25 μm/min (n = 11) after contact (Fig. 5D). This was primarily because of the decrease in cell population migrating at a velocity of more than 3 μm/min and increase in cells migrating backward (Fig. 5E). Nevertheless, LP-th cells predominantly and continuously migrated forward after contact with DM-th cells.

LP-lu cells migrated forward at a high speed (average velocity of 1.20 ± 0.29 μm/min; n = 11) before contact with DM-th cells (Fig. 5D). After contact with DM-th cells, the average velocity of LP-lu cell leading edges was −0.03 ± 0.15 μm/min (n = 11) (Fig. 5D). These cells did not cease to migrate, but approximately half of the cells began to migrate backward (Fig. 5F). Leading edges migrating forward at a velocity of more than 2 μm/min decreased, whereas leading edges of cells migrating backward at low speed (less than 1 μm/min) increased on contact with DM-th cells (Fig. 5F).

2.7. Behavior of lumbar DM (DM-lu) cells co-cultured with LP-lu cells

DM-lu cells migrated forward at a high speed (average velocity of 1.46 ± 0.29 μm/min; n = 11) before contact with LP-lu cells (Fig. 6A). Thirty minutes before contact with LP-lu cells, more than half of DM-lu cells migrated forward at a velocity of more than 2 μm/min, whereas approximately 50% of cells migrated backward after contact (Fig. 6B). Only in the combination of this co-culture, the leading edges of DM-lu cells migrated only slightly after contact (average velocity of 0.14 ± 0.20 μm/min; n = 11) (Fig. 3E, 6B).

2.8. Behavior of LP-lu cells co-cultured with DM-lu cells

LP-lu cells migrated forward (average velocity of 0.49 ± 0.23 μm/min; n = 11) before contact with DM-lu cells (Fig. 6C). Approximately 70% of LP-lu cells migrated forward within 30 min before contact (Fig. 6D). After contact with DM-lu

cells, approximately 70% of LP-lu cells migrated backward, which decreased to approximately 40% at 30 min after contact (Fig. 6D). LP-lu cells migrated backward, but on contact with another LP cell behind it, the cells changed the direction of migration again in seven of 11 cases.

2.9. Behavior of SC-lu cells

We tried to perform experiments using SC-lu cells. However, SC-lu cells hardly migrated to make contact with other cells (data not shown).

2.10. Alteration in somite cell size before and after contact with LP cells

Fig. 7 shows the cell length between the leading and trailing edges of cells after contact compared to that before contact in each examination. After contact with LP-lu cells, the length of both SC-th and DM-th cells reduced remarkably. On contact with LP-th cells, the length of SC-th and DM-th cells did not virtually change before and after contact. The length of DM-lu cells also did not change on contact with LP-lu cells.

2.11. Grouping velocity distribution patterns by hierarchical clustering analysis

As shown in Figs. 4–6, somite and LP cells migrated at varying velocity distribution patterns based on the combination of their co-culture (Fig. 4B, C, E, F; 5B, C, E, F; 6B, D). Clustering analysis revealed that velocity distribution patterns were divided into three groups (Fig. 8A), and distinctive features were observed in all velocity distribution patterns (Fig. 8B). CL1 (cluster one) was characterized by forward migration at more than 1 μm/min. In CL2, the cells migrated forward at low velocity. In CL3, the proportion of backward migration was high.

SC and DM cells predominantly migrated forward before contact (Fig. 8C, 2nd line; CL1). The direction of migration of somite cells changed to backward after contact with LP cells (Fig. 8C, 3rd, 5th, 7th, and 9th columns; CL3), except for SC-th cells

that continuously migrated forward (CL2) after contact with LP-th cells (Fig. 8C, 1st column).

Although migration of DM-th cells after contact with LP-lu cells was grouped under CL2 (Fig. 8C, 7th column), 16.7% of DM-th cells migrated backward at a velocity of more than 3 μm/min (Fig. 4C), indicating that a considerable number of DM-th cells migrated backward, unlike other cells grouped in CL2 (Fig. 8A, heatmap).

On contact with SC-th cells, LP-th cells changed the direction of migration (Fig. 8C, 2nd column). Before contact, LP-th cells migrated forward at a high velocity (CL1), but the cells migrated backward after contact (CL3). On the contrary, LP-lu cells always migrated forward (CL1 and CL2) before and after contact with SC-th cells (Fig. 8C, 4th column). After contact with DM-lu cells, LP-lu cells transiently changed the direction of migration to backward (CL3) and then again to forward at low velocity (CL2) (Fig. 8C, 10th column).

3. Discussion

A major portion of the axial skeleton of vertebrates is derived from somites. They form various bones along the rostro-caudal axis, from the occipital bone to the coccygeal bone. Of these somites, thoracic somites particularly form long ribs in addition to the thoracic vertebrae. As shown by Kieny et al. (1972), although thoracic somites specifically form the ribs, their length depends on the neighboring conditions (Kieny et al., 1972). When the thoracic segmental plate is ectopically transplanted into the cervical region, the transplants form vertebral ribs but no sternal ribs.

For rib formation, thoracic somite cells penetrate into the somatic lateral plate mesoderm. When the thoracic somite mesoderm is transplanted into the lumbar region, it does not penetrate into the lumbar somatic mesoderm and forms short ribs (Matsumori et al., unpublished data). We hypothesized that the intercellular interaction between somite and LP cells could control cell behavior to form the axial skeleton.

Here, we present the migratory behavior of somite and somatic LP cells in an *in vitro* co-culture system and showed that SC-th cells tended to continuously migrate forward after contact with LP-th cells, whereas they migrated in the reverse direction

after contact with LP-lu cells.

Embryonic cells isolated *in vitro* may change their developmental fate, which would misinterpret our findings. In fact, the epithelial somite develops depending on its surrounding tissues. The surface ectoderm induces the DM and notochord, and the floor plate induces the SC. Even if each somitic primordium is combined with an ectopic tissue, it develops according to the tissue in contact (Aoyama and Asamoto, 1988; Ordahl and Le Douarin, 1992; Christ et al., 1992; Pourquié et al., 1993; Aoyama, 1993; Christ and Ordahl, 1995; Williams and Ordahl, 1997; Dockter and Ordahl, 2000; Monsoro-Burq, 2005). However, as we have shown, the caudal third somite (stage III somite) begins to differentiate and at least some part of it cannot change its fate after being rotated dorsoventrally (Aoyama and Asamoto, 1988). The presumptive dermomyotomal region and a part of the presumptive sclerotomal region of the somite differentiate along their original fate under heterotopic circumstances. Furthermore, except for stage I–III somites, isolated somites differentiate into cartilage tissue and muscle fibers without induction of other tissues *in vitro* (Ellison et al., 1969a, 1969b; Kenny-Mobbs and Thorogood, 1987; Buffinger and Stockdale, 1994; Stern and Hauschka, 1995). We did not use stage I–III somites in the present study. Thus, the somite cells that we investigated *in vitro* were considered to retain their fate and represent their behavior *in vivo*.

In the present study, we primarily used the 1D migratory system instead of the 2D system because of simplicity of analysis of cell migratory behavior. It has been reported that there is no considerable difference in neural crest cell behavior and migratory abilities between the 1D and 2D systems, although speed and directionality were slightly less in the 1D system than those in the 2D system (Scarpa et al., 2013, 2016). The velocity of SC-th cells co-cultured with LP-th cells was 1.36 ± 0.23 μm/min (n = 11) (Fig. 4A), of DM-th cells co-cultured with LP-th cells was 0.94 ± 0.32 μm/min (n = 11) (Fig. 5A), and of LP-th cells co-cultured with SC-th cells was 1.58 ± 0.39 μm/min (n = 11) (Fig. 4D). Our results almost agree with the velocities of SC (1.095 μm/min), DM (1.085 μm/min), and LP (1.925 μm/min) cells reported by Bellairs et al. (1980) at the interval of 12 s (Bellairs et al., 1980).

We found that SC cells changed the direction of migration just after contact with LP-lu cells, suggesting that the effect of intercellular interaction is not based on

long-range mechanisms, such as chemotaxis, haptotaxis, or contact guidance, but on cell–cell contact. After contact with LP-th cells, SC-th cells, which form the rib anlagen, continued migrating in the same direction as that before contact (Fig. 8C, 1st column). However, SC-th cells migrated in the opposite direction after contact with LP-lu cells (Fig. 8C, 3rd column). Abercrombie and Heaysman (1954) reported that contact inhibition results in restriction of the velocity of cells and changes the direction of cell migration (Abercrombie and Heaysman, 1954). A series of studies has reported that cell–cell contact affects the behavior of cells. Eph family ligands guide the migration of neural crest cells and motor axon from the neural tube (Wang and Anderson, 1997). Drosophila macrophages undergo contact repulsion and disperse laterally to form a "three-lined" organization pattern from a linear cellular array at the ventral midline (Stramer et al., 2010; Davis et al., 2012; Davis et al., 2015). Neural crest cells migrate in an N-cadherin/CIL-dependent mechanism (Erickson, 1985; Carmona-Fontaine et al., 2008; Theveneau et al., 2010; Scarpa et al., 2015). In these studies, the behaviors of cells were analyzed *in vitro* and were confirmed *in vivo*.

To form the ribs, SC-th cells start to migrate ventrolaterally while proliferating, and then penetrate into the somatopleure. When SC-th cells contact LP-th cells, they continued to migrate forward at a velocity of 0.46 ± 0.15 μm/min (n = 11; Fig. 4A). After migrating for 7.5 days at this velocity, the migrated distance would be 4.97 mm, which is almost the same length as the 4th vertebral rib, 4.95 ± 0.18 mm (n = 10) at HH-stage 36 (approximately 10 days after incubation). This finding suggests that cell migration speed is a significant factor to determine the length of a rib, which may alternatively be affected by cell proliferation rate.

However, SC-th cells reversed the direction of migration after contact with LP-lu cells (Fig. 8C, 3rd column). At 0.55 ± 0.23 μm/min (n = 11), SC-th cells migrated away from LP-lu cells after contact (Fig. 4A). This phenomenon may represent the somite cell behavior *in vivo*. Ectopic transplantation of leg somatopleural mesoderm in the thoracic region alters the fate of somite descendant cells and causes the loss of sterno-distal ribs (Liem and Aoyama, 2009). Furthermore, we found that thoracic somite cells did not enter into the tissue derived from the lumbar lateral plate when the thoracic somite mesoderm was ectopically transplanted in the lumbar region (Matsumori et al., unpublished data). In normal development, SC-th cells can contact

LP-lu cells only at the thoraco–lumbar boundary. This repulsive nature of intercellular interaction observed in the present study would help to avoid malformation caused by penetration of rib-forming thoracic somite cells into the lumbar lateral plate by accident.

Burke and Nowicki (2003) proposed that the body wall should be classified into two categories, viz., primaxial and abaxial regions, according to the relationship between the somite and lateral plate mesoderm in the course of development (Burke and Nowicki, 2003). The domain comprising only somite cells is defined as the primaxial region, and the domain of the lateral plate with somite and lateral plate cells is defined as the abaxial region. They named the interface between the primaxial and the abaxial region as the lateral somitic frontier. At the thoracic level, the cluster of somite cell population elongates laterally into the lateral plate mesoderm to form the somitic bud (Christ et al., 1983). Furthermore, some somite cells migrate across the lateral somitic frontier and mix with LP cells (Nowicki et al., 2003). These somite cells constitute the abaxial region. We have previously reported that the rib in birds is composed of three compartments according to developmental dependencies on adjacent tissues (Aoyama et al., 2005). The proximal and vertebro-distal ribs correspond to the primaxial region, whereas the sterno-distal rib corresponds to the abaxial region (Burke and Nowicki, 2003). In the present study, although we could not distinguish primaxial and abaxial cells *in vitro*, both categories of cells have such common nature that they penetrate the lateral plate mesoderm at the thoracic level but not at the lumbar level. Consequently, in either case, our findings are consistent with the thoracic somite behavior *in vivo*.

We expected that DM-th cells would continuously migrate forward after contact with LP-th cells and migrate backward after contact with LP-lu cells, similar to that observed for SC-th cells. However, in our *in vitro* system, the migratory behavior of DM cells, which include the muscle anlagen, was different from that of SC-th cells, which include the rib anlagen. After contact with either LP-th or LP-lu cells, DM cells reversed the direction of migration (Fig. 8C, 5th, 7th, and 9th column).

In vivo, DM-th cells migrate adhering to each other to form intercostal muscles, whereas DM-lu cells migrate individually to form the limb muscles (Chevallier, 1979; Jacob et al., 1979). In the present study, the cells were individually analyzed *in vitro*. DM-th cells may be able to invade the tissue that repels because they migrate as a mass. Rovasio et al. (1983) showed that neural crest cells exhibited

oriented migration when they were cultured at high density, whereas they migrated randomly at a low density (Rovasio et al., 1983). Although DM is an epithelial tissue, a part of the somite undergoes epithelial–mesenchymal transition to form SC (Chal and Pourquié, 2017). After migration, SC-derived cells aggregate and finally form the cartilage, suggesting that SC cells migrate individually *in vivo*. The migratory behavior of SC-derived cells *in vitro* shown in this study may reflect the pattern observed *in vivo*.

This study showed that the behaviors of rib-forming SC-th cells were significantly different depending on whether the cells made contact with LP-th or LP-lu cells. SC-th cells migrated backward after contact with LP-lu cells. This phenomenon was considered to be caused by contact of thoracic somite cells with LP-lu cells. In normal development, chicken ribs grow laterally/ventrally, and then the sterno-distal ribs form pointing cranially but never enter the caudal–lumbar region. This may be explained by the repulsive intercellular interaction, which prevents SC-th cells from entering the lumbar somatic lateral plate. Thus, the cell–cell interaction presented here would assure that the rib forms only in the thoracic region.

4. Experimental procedures

4.1. Preparation of embryos

Fertilized eggs of White Leghorn chick were purchased from a local farm and incubated at 38°C in a humidified incubator.

4.2. Isolation of explants from embryos

In the present study, “thoracic” indicated the 22nd–25th somite level, including the 3rd–6th pairs of rib anlagen, and possessed both vertebral and sternal ribs. “Lumbar” indicated the 29th–31st somite level, where somites form the 3rd–6th lumbosacral vertebrae. A part of the embryo with the desired embryonic tissues was dissected and treated with 500 IU/mL dispase (Godo Shusei, Japan) in culture medium at 37°C for 15–30 min, followed by isolation of each tissue using sharpened tungsten needles in

Tyrode's saline. For culturing the cells, we used a 1:1 mix of of Dulbecco's modified Eagle's medium (DMEM; Sigma-Aldrich) and Ham's F-10 (F10; Sigma-Aldrich), supplemented with 10% fetal calf serum (FCS) and 100 μg/mL kanamycin sulfate. A piece of SC was separated from DM. Although DM was separated carefully from SC, some SC cells may remain in the excised DM. Because SC is a mesenchymal tissue, it was difficult to remove it without destruction. Lateral half of DM was obtained by sagittally cutting DM in the middle. To isolate the somatic LP, it was cut at the border of somatic and splanchnic LP. SC-th and thoracic lumbar thoracic somatic lateral plate (LP-th) were dissected from HH-stage (Hamburger and Hamilton 1951) 17–18 (29–37 somite stage) chick embryo. DM-th and LP-lu were dissected from HH-stage 17–20 (29–41 somite stage) chick embryo.

4.3. Fluorescence staining

To trace cells *in vitro*, each explant was labeled with DiI or DiO (Invitrogen). The stock dye solutions (0.05%) were added to the culture medium at a final concentration of 0.01%. The culture medium consisted of DMEM:F10 = 1:1 supplemented with 10% FCS and 100 μg/mL kanamycin sulfate. The isolated tissues were incubated in the dye solution at 37°C in 5% CO_2/air for 20 min, followed by rinsing five times with Tyrode's saline to remove unconjugated dye.

4.4. Co-culture experiment on a 2D substrate

Explants of somites and its derivatives were co-cultured with explants of LP in a glass-base dish (3911-035 Iwaki, Japan) with the culture medium at 37°C under 5% CO_2/air. A pair of explants was placed with a spacing of 1 mm between the explants. The explants settled and proliferated on the substrate. Cells migrated away from the explants and made contact with each other halfway between the explants.

4.5. Co-culture experiment on a 1D substrate

The explants were co-cultured in a semisolid medium on CytoGraph (DNP, Japan) type L10S300 with 10-μm wide hydrophilic paths intervening with 300-μm wide hydrophobic areas. The semisolid medium was composed of DMEM:F10 = 1:1, 15% FCS, 100 μg/mL kanamycin sulfate, and 1.7% methylcellulose 4000 (Chameleon Reagent). The hydrophobic areas were constructed by coating with tetraethyleneglycol layer, and hydrophilic paths were uncovered glass surface (Okochi et al. 2009). The substrate was treated with 3% bovine serum albumin (Sigma-Aldrich) for blocking excess cell adhesion before culture.

4.6. Time-lapse imaging

The cultured cells were observed under a phase-contrast microscope (IX71, Olympus, Japan) with a 4× or 10× objective and photographed every 1 min for 48 h with a camera (Eos Kiss X6i, Canon, Japan) controlled by EOS Utility (Canon, Japan).

4.7. Cell tracking

We analyzed cell migration using consecutive photographs captured every 10 min for 60 min before and after contact between the co-culture cells. The cultured cells migrated away from the explants; co-cultured cells approached each other, and finally made contact. In this study, we named the preceding tip of the migrating cell as the leading edge and the rear tip as the trailing edge. These names were defined according to the initial direction of cell migration and we did not rename when the cells changed their direction of migration. On consecutive photographs, we manually marked the leading and trailing edges (Fig. 2D), and their positions were recorded in X–Y coordinates of pixels using ImageJ Multi-point Analyze Tool (NIH, USA). Then, we calculated the migration velocity (μm/min) from the distance between the marked points using Numbers (Apple) and Excel (Microsoft).

4.8. Statistical analysis

Statistical analysis was performed using R (R Development Core Team,

Vienna, Austria). The migration velocity was compared by Student's t-test ($P > 0.05$, by F test) or the Wilcoxon rank sum test ($P \leq 0.05$, by F test). Comparison of the direction of migration was performed using the Mardia–Watson–Wheeler test for homogeneity using R. We divided each 60-min period before and after contact into two periods of 30 min each. Velocity distribution patterns in each period were grouped by hierarchical clustering analysis using the Ward's method. The Ward's method is an agglomerative method based on a sum of squares criterion (Murtagh and Legendre, 2014). Observations in each cluster were agglomerated to minimize the extra sum of squares at each clustering step. Distance obtained by criterion of the Ward's method represented the height of dendrograms.

Acknowledgments

A part of this work was supported by JSPS KAKENHI Grant Numbers JP26460254, JP23590219.

Conflicts of interest

The authors declare no conflict of interest.

References

Abercrombie, M. and Heaysman, J.E.M., 1954. Observations on the social behaviour of cells in tissue culture. II. Monolayering of fibroblasts. Exp. Cell Res. 6, 293–306. https://doi.org/10.1016/0014-4827(54)90176-7

Aoyama, H., 1993. Developmental plasticity of the prospective dermatome and the prospective sclerotome region of an avian somite. Develop. Growth Differ. 35, 507–519. https://doi.org/10.1111/j.1440-169X.1993.00507.x

Aoyama, H. and Asamoto, K., 1988. Determination of somite cells: independence of cell-differentiation and morphogenesis. Development 104, 15–28.

Aoyama, H. and Asamoto, K., 2000. The developmental fate of the rostral/caudal half of a somite for vertebra and rib formation: experimental confirmation of the resegmentation

theory using chick-quail chimeras. Mech. Dev. 99, 71–82. https://doi.org/10.1016/S0925-4773(00)00481-0

Aoyama, H., Mizutani-Koseki, Y. and Koseki, H., 2005. Three developmental compartments involved in rib formation. Int. J. Dev. Biol. 49, 325–333. https://doi.org/10.1387/ijdb.041932ha

Bellairs, R., Sanders, E.J. and Portch, P.A., 1980. Behavioural properties of chick somitic mesoderm and lateral plate when explanted *in vitro*. J. Embryol. Exp. Morphol. 56, 41–58.

Buffinger, N. and Stockdale, F.E., 1994. Myogenic specification in somites: induction by axial structures. Development 120, (6) 1443–1452.

Burke, A.C. and Nowicki, J.L., 2003. A new view of patterning domains in the vertebrate mesoderm. Dev. Cell 4, 159–165. https://doi.org/10.1016/S1534-5807(03)00033-9

Carmona-Fontaine, C., Matthews, H.K., Kuriyama, S., Moreno, M., Dunn, G.A., Parsons, M., Stern, C.D. and Mayor, R., 2008. Contact inhibition of locomotion *in vivo* controls neural crest directional migration. Nature 456, 957–961. https://doi.org/10.1038/nature07441

Carter, S.B., 1965. Principles of cell motility: the direction of cell movement and cancer invasion. Nature 208, 1183–1187. https://doi.org/10.1038/2081183a0

Chal, J. and Pourquié, O., 2017. Making muscle: skeletal myogenesis *in vivo* and *in vitro*. Development 144, 2104–2122. https://doi.org/10.1242/dev.151035

Chevallier, A., 1979. Role of the somitic mesoderm in the development of the thorax in bird embryos. II. Origin of thoracic and appendicular musculature. J. Embryol. Exp. Morphol. 49, 73–88.

Christ, B., Brandsaberi, B., Grim, M. and Wilting, J., 1992. Local signaling in dermomyotomal cell type specification. Anat. Embryol. 186, 505–510.

Christ, B., Jacob, M. and Jacob, H.J., 1983. On the origin and development of the ventrolateral abdominal muscles in the avian embryo. An experimental and ultrastructural study. Anat. Embryol. 166, 87–101.

Christ, B. and Ordahl, C.P., 1995. Early stages of chick somite development. Anat. Embryol. 191, 381–396. https://doi.org/10.1007/BF00304424

Cousin, H., 2017. Cadherins function during the collective cell migration of Xenopus cranial neural crest cells: revisiting the role of E-cadherin. Mech. Dev. 148, 79–88. https://doi.org/10.1016/j.mod.2017.04.006

Davis, J.R., Huang, C.Y., Zanet, J., Harrison, S., Rosten, E., Cox, S., Soong, D.Y., Dunn, G.A. and Stramer, B.M., 2012. Emergence of embryonic pattern through contact inhibition of locomotion. Development 139, 4555–4560. https://doi.org/10.1242/dev.082248.

Davis, J.R., Luchici, A., Mosis, F., Thackery, J., Salazar, J.A., Mao, Y.L., Dunn, G.A., Betz, T., Miodownik, M. and Stramer, B.M., 2015. Inter-Cellular Forces Orchestrate Contact Inhibition of Locomotion. Cell 161, 361–373. http://dx.doi.org/10.1016/j.cell.2015.02.015.

de la Loza, M.C.D., Diaz-Torres, A., Zurita, F., Rosales-Nieves, A.E., Moeendarbary, E., Franze, K., Martin-Bermudo, M.D. and Gonzalez-Reyes, A., 2017. Laminin levels regulate tissue migration and anterior-posterior polarity during egg morphogenesis in Drosophila. Cell Rep. 20, 211–223. http://dx.doi.org/10.1016/j.celrep.2017.06.031

Dockter, J. and Ordahl, C.P., 2000. Dorsoventral axis determination in the somite: a re-examination. Development 127, 2201–2206.

Ellison, M.L., Ambrose, E.J. and Easty, G.C., 1969a. Chondrogenesis in chick embryo somites *in vitro*. J. Embryol. Exp. Morphol. 21, 331–340.

Ellison, M.L., Ambrose, E.J. and Easty, G.C., 1969b. Myogenesis in chick embryo somites *in vitro*. J. Embryol. Exp. Morphol. 21, 341–346.

Erickson, C.A., 1985. Control of neural crest cell dispersion in the trunk of the avian embryo. Dev. Biol. 111, 138–157. https://doi.org/10.1016/0012-1606(85)90442-7

Hamburger, V. and Hamilton, H.L., 1951. A series of normal stages in the development of the chick embryo. J. Morphol. 88, 49–92. https://doi.org/10.1002/jmor.1050880104

Hernandez-Fleming, M., Rohrbach, E.W. and Bashaw, G.J., 2017. Sema-1a reverse signaling promotes midline crossing in response to secreted semaphorins. Cell Rep. 18, 174–184. http://dx.doi.org/10.1016/j.celrep.2016.12.027

Huang, R.J., Zhi, Q.X., Schmidt, C., Wilting, J., Brand-Saberi, B. and Christ, B., 2000. Sclerotomal origin of the ribs. Development 127, 527–532.

Jacob, M., Christ, B. and Jacob, H.J., 1979. The migration of myogenic cells from the somites into the leg region of avian embryos. Anat. Embryol. (Berl) 157, 291–309.

Jotereau, F.V. and Le Douarin, N.M., 1982. Demonstration of a cyclic renewal of the lymphocyte precursor cells in the quail thymus during embryonic and perinatal life. J. Immunol. 129, 1869–1877.

Kato, N. and Aoyama, H., 1998. Dermomyotomal origin of the ribs as revealed by extirpation and transplantation experiments in chick and quail embryos. Development 125, 3437–3443.

Kennymobbs, T. and Thorogood, P., 1987. Autonomy of differentiation in avian brachial somites and the influence of adjacent tissues. Development 100, 449–462.

Kieny, M., Sengel, P. and Mauger, A., 1972. Early regionalization of somitic mesoderm as studied by development of axial skeleton of chick-embryo. Dev. Biol. 28, 142–161. https://doi.org/10.1016/0012-1606(72)90133-9

Kridsada, K., Niu, J.W., Haldipur, P., Wang, Z.P., Ding, L., Li, J.J., Lindgren, A.G., Herrera, E., Thomas, G.M., Chizhikov, V.V., Millen, K.J. and Luo, W.Q., 2018. Roof plate-derived radial glial-like cells support developmental growth of rapidly adapting mechanoreceptor ascending axons. Cell Rep. 23, 2928–2941. https://doi.org/10.1016/j.celrep.2018.05.025

Laumonnerie, C., Tong, Y.G., Alstermark, H. and Wilson, S.I., 2015. Commissural axonal corridors instruct neuronal migration in the mouse spinal cord. Nat. Commun. 6, 7028, 1–14. https://doi.org/10.1038/ncomms8028

Le Douarin, N.M., 1984. Cell migrations in embryos. Cell 38, 353–360.

Liem, I.K. and Aoyama, H., 2009. Body wall morphogenesis: limb-genesis interferes with body wall-genesis via its influence on the abaxial somite derivatives. Mech. Dev. 126, 198–211. https://doi.org/10.1016/j.mod.2008.11.003

Mayor, R. and Etienne-Manneville, S., 2016. The front and rear of collective cell migration. Nat. Rev. Mol. Cell Bio. 17, 97–109. https://doi.org/10.1038/nrm.2015.14

Monsoro-Burq, A.H., 2005. Sclerotome development and morphogenesis: when experimental embryology meets genetics. Int. J. Dev. Biol. 49, 301–308. https://doi.org/10.1387/ijdb.041953am

Murtagh, F. and Legendre, P., 2014. Ward's hierarchical agglomerative clustering method: which algorithms implement Ward's criterion? J. Classif. 31, 274–295. https://doi.org/10.1007/s00357-014-9161-z

Nowicki, J.L. and Burke, A.C., 2000. Hox genes and morphological identity: axial versus lateral patterning in the vertebrate mesoderm. Development 127, 4265–4275.

Nowicki, J.L., Takimoto, R. and Burke, A.C., 2003. The lateral somitic frontier: dorso-ventral aspects of anterio-posterior regionalization in avian embryos. Mech. Dev. 120, 227–240. https://doi.org/10.1016/S0925-4773(02)00415-X

Okochi, N., Okazaki, T. and Hattori, H., 2009. Encouraging effect of cadherin-mediated cell-cell Junctions on Transfer Printing of micropatterned vascular endothelial cells. Langmuir 25, 6947–6953. https://doi.org/10.1021/la9006668.

Ordahl, C.P. and Le Douarin, N.M., 1992. Two myogenic lineages within the developing somite. Development 114, 339–353.

Pourquié, O., Coltey, M., Teillet, M.A., Ordahl, C. and Le Douarin, N.M., 1993. Control of dorsoventral patterning of somitic derivatives by notochord and floor plate. PNAS. 90, 5242–5246. https://doi.org/10.1073/pnas.90.11.5242

Reig, G., Pulgar, E. and Concha, M.L., 2014. Cell migration: from tissue culture to embryos. Development 141, 1999–2013. https://doi.org/10.1242/dev.101451

Rovasio, R. A., Delouvee, A., Yamada, K. M., Timpl, R., Thiery, J.P., 1983. Neural crest cell migration: requirements for exogenous fibronectin and high cell density. J. Cell Biol. 96, 462–473. https://doi.org/10.1083/jcb.96.2.462

Scarpa, E. and Mayor, R., 2016. Collective cell migration in development. J. Cell Biol. 212, 143–155. https://doi.org/10.1083/jcb.201508047

Scarpa, E., Roycroft, A., Theveneau, E., Terriac, E., Piel, M. and Mayor, R., 2013. A novel method to study contact inhibition of locomotion using micropatterned substrates. Biol. Open 2, 901–906. https://doi.org/10.1242/bio.20135504

Scarpa, E., Roycroft, A., Theveneau, E., Terriac, E., Piel, M. and Mayor, R., 2016. A novel method to study contact inhibition of locomotion using micropatterned substrates (vol 2, pg 901). Biol. Open 5, 1553–1553. https://doi.org/10.1242/bio.020917

Scarpa, E., Szabo, A., Bibonne, A., Theveneau, E., Parsons, M. and Mayor, R., 2015. Cadherin switch during EMT in neural crest cells leads to contact inhibition of locomotion via repolarization of forces. Dev. Cell 34, 421–434. http://dx.doi.org/10.1016/j.devcel.2015.06.012

Shearman, R.M. and Burke, C., 2009. The lateral somitic frontier in ontogeny and phylogeny. J. Exp. Zool. Part B. 312B, 603–612. https://doi.org/10.1002/jez.b.21246

Stern, H.M. and Hauschka, S.D., 1995. Neural tube and notochord promote *in vitro* myogenesis in single somite explants. Dev. Biol. 167, 87–103. https://doi.org/10.1006/dbio.1995.1009

Stramer, B., Moreira, S., Millard, T., Evans, I., Huang, C.Y., Sabet, O., Milner, M., Dunn, G., Martin, P. and Wood, W., 2010. Clasp-mediated microtubule bundling regulates persistent motility and contact repulsion in Drosophila macrophages *in vivo*. J. Cell Biol. 189, 681–689. https://doi.org/10.1083/jcb.200912134

Sudo, H., Takahashi, Y., Tonegawa, A., Arase, Y., Aoyama, H., Mizutani-Koseki, Y., Moriya, H., Wilting, J., Christ, B. and Koseki, H., 2001. Inductive signals from the somatopleure mediated by bone morphogenetic proteins are essential for the formation of the sternal component of avian ribs. Dev. Biol. 232, 284–300. https://doi.org/10.1006/dbio.2001.0198

Takeichi, M., 2014. Dynamic contacts: rearranging adherens junctions to drive epithelial remodelling. Nat. Rev. Mol. Cell Bio. 15, 397–410. https://doi.org/10.1038/nrm3802

Theveneau, E., Marchant, L., Kuriyama, S., Gull, M., Moepps, B., Parsons, M. and Mayor, R., 2010. Collective chemotaxis requires contact-dependent cell polarity. Dev. Cell 19, 39–53. https://doi.org/10.1016/j.devcel.2010.06.012

Villar-Cervino, V., Molano-Mazon, M., Catchpole, T., Valdeolmillos, M., Henkemeyer, M., Martinez, L.M., Borrell, V. and Marin, O., 2013. Contact repulsion controls the dispersion and final distribution of Cajal-Retzius cells. Neuron 77, 457–471. http://dx.doi.org/10.1016/j.neuron.2012.11.023

Wang, H.U. and Anderson, D.J., 1997. Eph family transmembrane ligands can mediate repulsive guidance of trunk neural crest migration and motor axon outgrowth. Neuron 18, 383–396. https://doi.org/10.1016/S0896-6273(00)81240-4

Williams, B.A. and Ordahl, C.P., 1997. Emergence of determined myotome precursor cells in the somite. Development 124, 4983–4997.

Figure captions

Fig. 1 Behavior of somite cell before and after contacting lateral plate cells on a conventional two-dimensional substrate. (A and B) Phase-contrast consecutive images. (A) Thoracic somite cells (white arrowhead) did not change the direction of migration for several minutes after contact with LP-th cells. (B) Thoracic somite cells (blue arrow) changed the direction of migration immediately after contact with LP-lu cells. (C and D) Diagrams show the direction of somite cell migration. The direction of somite cell migration was defined by an angle to the reference line from the somite to the lateral plate explants. The direction to the lateral plate explant is indicated as zero degree. The cells were tracked manually. Polar plot was graphed using the code written by Karsten D Bjerre (2002). The direction of somite cell migration for 100 min before and after first contact with lateral plate cells was compared by the Mardia–Watson–Wheeler test for homogeneity using R. (C) Thoracic somites were co-cultured with LP-th cells, and 13 of them were recorded before they made contact. Before contact, most thoracic somite cells migrated toward the thoracic lateral plate explant. After contact, 4 of the 13 cells became obscure, although somite cells more or less changed the direction of migration, most cells appeared to migrate along nearly the same direction as that before contact. (D) Thoracic somites were co-cultured with LP-lu cells. After contact, 3 of the 12 cells became obscure, most somite cells appeared to change the direction of migration. They migrated toward LP-lu explant before they made contact with LP cells. Abbreviations: LP, somatic lateral plate; -th, thoracic; -lu, lumbar.

Fig. 2 Cell migration on a one-dimensional substrate, the CytoGraph. (A) SC and LP fragments were isolated from chick embryos and explanted on the opposite side of the cytophilic pathways [upper three pathways in (A) indicated with blue lines], which were 10-µm wide with 300-µm cytophobic intervals. SC (magenta arrow) and LP cells (green arrow) migrated away from the explants and continued to migrate along the cytophilic pathways. (B and C) Consecutive photos of SC cells and LP cells migrating from the opposite ends of the cytophilic pathways. Photos were captured every 10 min for 60 minutes before (negative values) and after (positive values) cells made contact

with each other. (B) SC-th and LP-th cells were co-cultured. SC-th cells stopped migration after contact with LP-th cells. (C) SC-th and LP-lu cells were co-cultured. SC-th cells migrated in the reverse direction after contact with LP-lu cells. (D) Definition of the leading and the trailing edge in the migrating cell. Abbreviations: SC, sclerotome; LP, somatic lateral plate; -th, thoracic; -lu, lumbar.

Fig. 3 Position of two co-cultured cells migrating from the opposite side on a one-dimensional substrate. Each line represents a cell with leading and trailing edges (x-axis), which were determined according to the contact point. Lines of the same color represent the same cell in each figure. (A) SC-th and LP-th cells were co-cultured five times (N = 5), and 11 pairs of cells were recorded (n = 11). (B) SC-th and LP-lu cells (N = 5; n = 11). (C) DM-th and LP-th cells (N = 3; n = 11). (D) DM-th and LP-lu cells (N = 5; n = 11). (E) DM-lu and LP-lu cells (N = 5; n = 11). We eliminated the data from cells when their trailing edge was too obscure to determine. Abbreviations: SC, sclerotome; LP, somatic lateral plate; DM, dermomyotome; -th, thoracic; -lu, lumbar.

Fig. 4 Change in the migration velocity of SC-th and LP-th or LP-lu cells before and after contact with each other on the one-dimensional substrate. Velocity was represented as that of the leading edge of migrating cells and calculated every 10 min. (A and D) Changes in average velocity of the cell 60 min before and after contact with its counterpart. (B, C, E, F) Horizontal stacked bar charts represent the percentage of cumulative cell numbers migrating at the velocity indicated above the chart. (A) SC-th cells continued to migrate at a lower velocity after contact with LP-th cells (n = 11) but changed the direction of migration after contact with LP-lu cells (n = 11). (B) Forward migrating SC-th cells decreased slightly to approximately 60% after contact with LP-th cells. (C) After contact with LP-lu cells, backward migration of SC-th cells increased notably. (D) LP-th cells changed the direction of migration after contact with SC-th cells, whereas LP-lu cells continued to migrate after contact with SC-th cells. (E) After contact with SC-th cells, backward migration of LP-th cells increased notably. (F) Forward migration of LP-lu cells decreased slightly after contact with SC-th cells. Abbreviations: SC, sclerotome; LP, somatic lateral plate; -th, thoracic; -lu, lumbar; n.s.,

no significant difference; *P < 0.05; **P < 0.01; ***P < 0.001. Data are represented as means ± SE.

Fig. 5 Change in migration velocity of DM-th and LP-th or LP-lu cells before and after contact with each other on the one-dimensional substrate. The velocity was represented as that of the leading edge of migrating cells and was calculated every 10 min. (A and D) Changes in average velocity of the cell 60 min before and after contact with its counterpart. (B, C, E, F) Horizontal stacked bar charts represent the percentage of cumulative cell numbers migrating at the velocity indicated above the chart. (A) DM-th cells changed the direction of migration after contact with LP-th cells (n = 11), whereas the velocity of migration appeared to be very low after contact with LP-lu cells (n = 10). (B) Most DM-th cells changed the migration direction to backward after contact with LP-th cells. (C) More than half DM-th cells continued forward migration, whereas a certain number of cells began backward migration at a relatively high speed after contact with LP-lu cells. (D) LP-th cells continued to migrate at a lower velocity after contact with DM-th cells, whereas LP-lu cells appeared to cease migration after contact with DM-th cells. (E) After contact with DM-th cells, forward migration of LP-th cells decreased gradually. Just after contact, they continued to migrate forward (0–30 min). After 30–60 min, some cells began to migrate backward. (F) Forward migration of LP-lu cells decreased to approximately 50% after contact with DM-th cells, which resulted in very low average velocity as shown in D. Abbreviations: DM, dermomyotome; LP, somatic lateral plate; -th, thoracic; -lu, lumbar; n.s., no significant difference; *P < 0.05; **P < 0.01; ***P < 0.001. Data are represented as means ± SE.

Fig. 6 Change in migration velocity of DM-lu and LP-lu cells before and after contact with each other on the one-dimensional substrate. Velocity was represented as that of the leading edge of migrating cells and calculated every 10 min. (A and C) Change in the average velocity of cells 60 min before and after contact with its counterpart. (B and D) Horizontal stacked bar charts represent the percentage of cumulative cell numbers migrating at the velocity indicated above the chart. (A) DM-lu cells appeared to continue migration at a lower velocity after contact with LP-lu cells (n = 11). (B)

Just after contact with LP-lu cells, a certain number of DM-lu cells began to migrate backward at a relatively high speed (more than 3 μm/min). The percentage of DM-lu cells migrating forward decreased once to approximately 50% 0–30 min after contact, and then it increased slightly in the following 30–60 min. (C) LP-lu cells changed the direction of migration after contact with DM-lu cells (n = 11). (D) The percentage of LP-lu cells migrating forward decreased once to approximately 30% 0–30 min after contact with DM-lu cells, and then it increased to approximately 60% in the following 30–60 min after contact. Just after contact (0–30 min), more than 70% of cells migrated backward, although most cells migrated at a relatively low velocity (0–1 μm/min). Abbreviations: DM, dermomyotome; LP, somatic lateral plate; -th, thoracic; -lu, lumbar; n.s., no significant difference; *P < 0.05; **P < 0.01; ***P < 0.001. Data are represented as means ± SE.

Fig. 7 The ratio of length of somite cells after contact with SC cells before contact. Cell length was measured from the leading edge to the trailing edge. To calculate the ratio of cell length, each cell length after the contact was divided by the average cell length of the cell before contact. The ratio of length of both SC-th and DM-th cells was significantly shorter when they made contact with LP-lu cells than that when they made contact with LP-th cells. Abbreviation; -th, thoracic; -lu, lumbar; SC, sclerotome; DM, dermomyotome; LP, lateral plate. Error bars denote SE. DM-th cells made contact with LP-lu cells, n = 10. n = 11, except for when DM-th cells made contact with LP-lu cells. n.s., no significant difference; *P < 0.01.

Fig. 8 Cluster analysis of migratory behavior. (A) Cluster dendrogram of velocity distribution of the cell. Height indicates criterion value in our agglomeration adapting the Ward's method. Heatmap represents the relative frequencies of cumulative cell numbers. White color indicates the maximum value. Clustering cells are indicated under the heatmap with co-cultured cells and with measured time period. (B) Difference in the velocity distribution pattern between clusters. In each cluster, we calculated the average of the relative frequencies of cells (percentage) migrating at each velocity indicated above the chart. (C) The time-course of changes in cell migration pattern are indicated by the cluster. Same clusters are indicated with the same

background color. For example, the migratory behavior of SC-th cells co-cultured with LP-th cells always belonged to CL1 or CL2, whereas those co-cultured with LP-lu cells changed from CL1 to CL3 after contact with LP-lu cells. Abbreviation; SC, sclerotome; DM, dermomyotome; LP, lateral plate; th, thoracic; lu, lumbar; B60, before 60–30 min; B30, before 30–0 min; A30, after 0–30 min; A60, after 30–60 min.

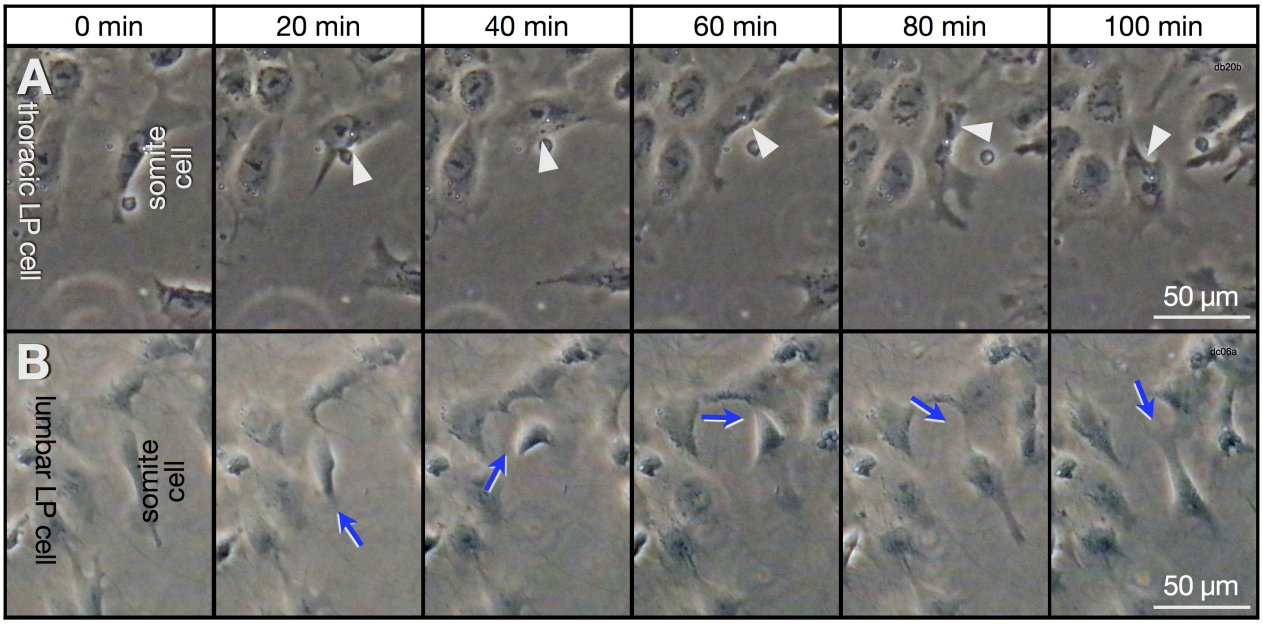
0 min
20 min
40 min
60 min
80 min
100 min
A
thoracic LP cell
somite cell
50 µm
B
lumbar LP cell
somite cell
50 µm

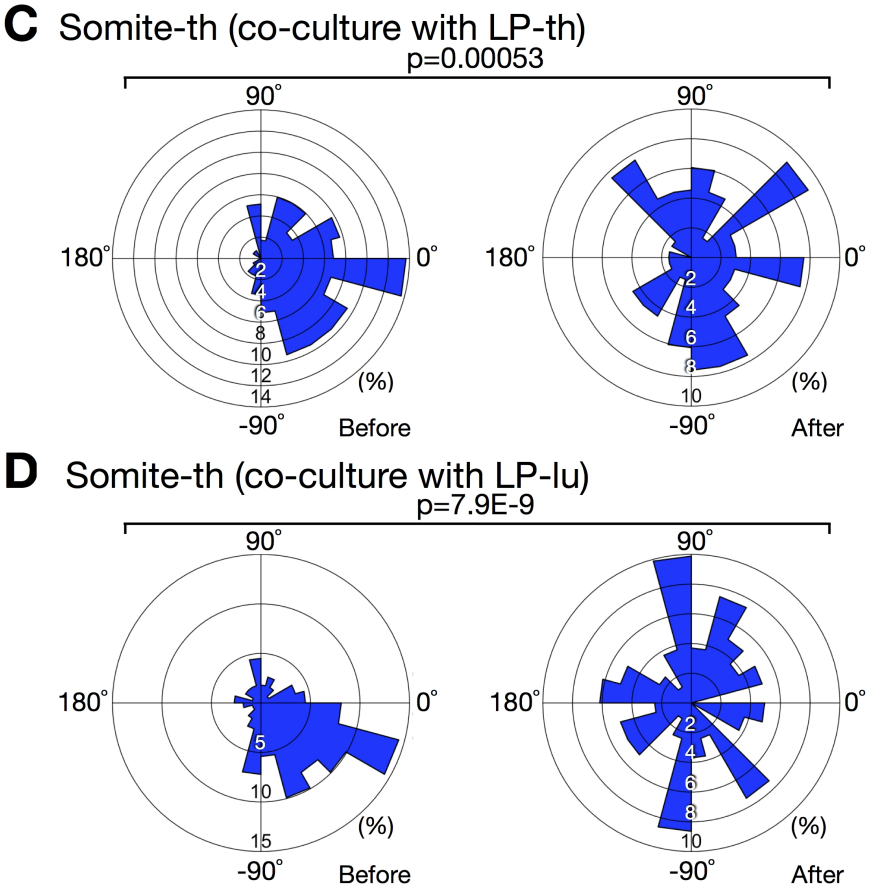
C Somite-th (co-culture with LP-th)
p=0.00053
90°
180°
0°
-90°
(%)
Before
After
D Somite-th (co-culture with LP-lu)
p=7.9E-9
90°
180°
0°
-90°
(%)
Before
After

Fig. 1

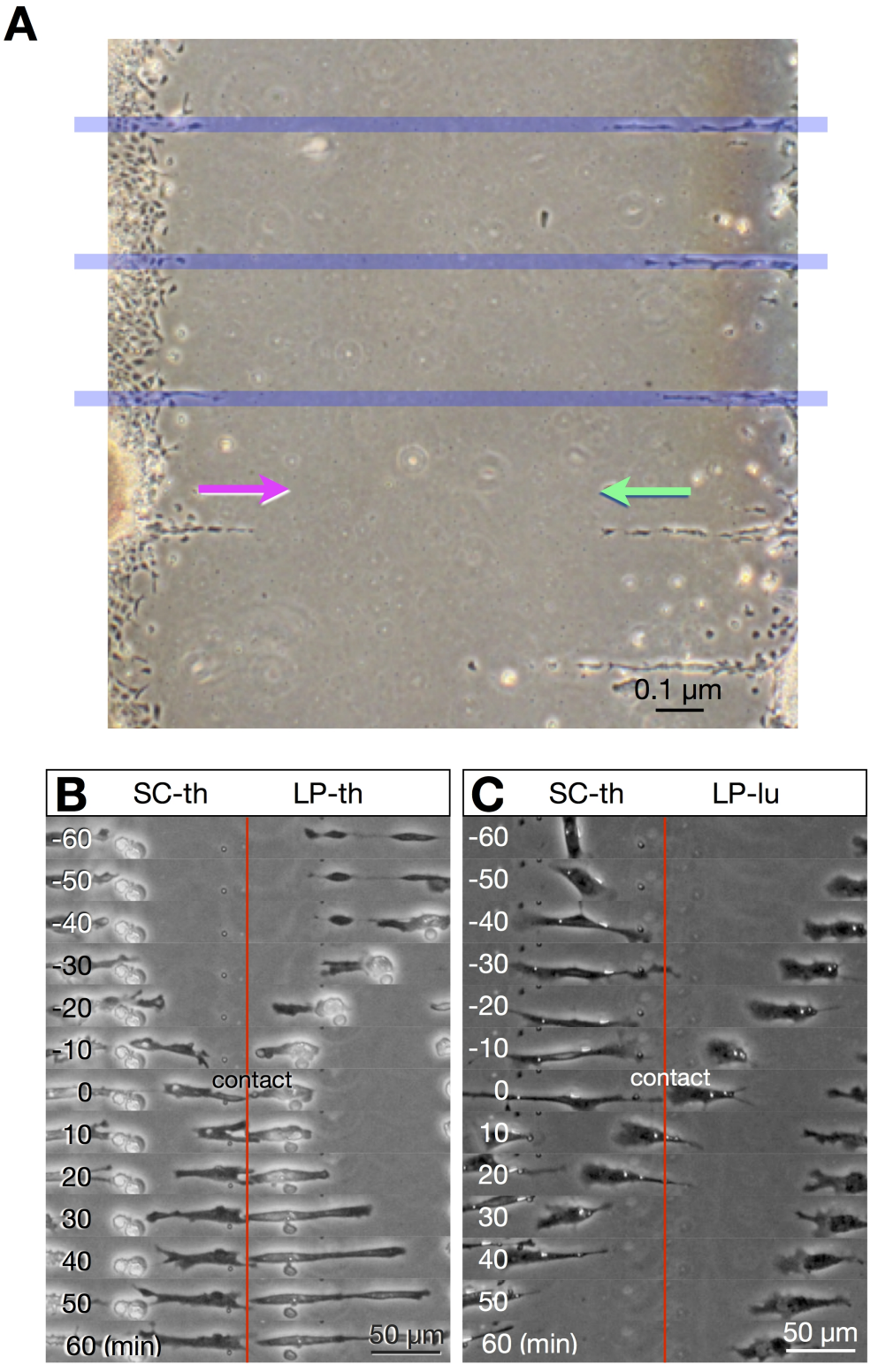
A
0.1 μm
B
SC-th
LP-th
-60
-50
-40
-30
-20
-10
0
10
20
30
40
50
60 (min)
contact
50 μm
C
SC-th
LP-lu
-60
-50
-40
-30
-20
-10
0
10
20
30
40
50
60 (min)
contact
50 μm
D
Somite cell
LP cell
axis
Trailing edge
Leading edge
Leading edge
Trailing edge

Fig. 2

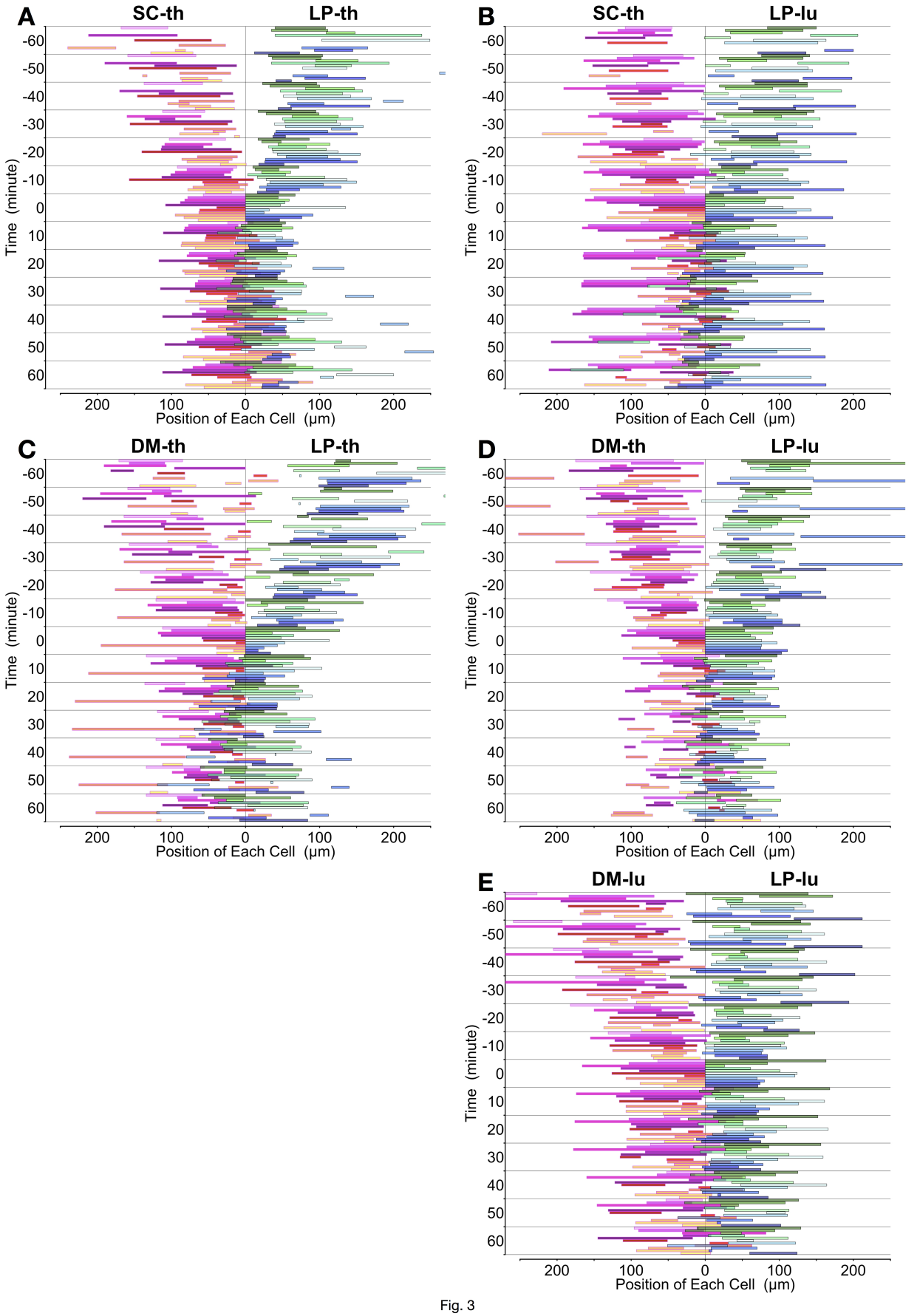
A
SC-th
LP-th
B
SC-th
LP-lu
C
DM-th
LP-th
D
DM-th
LP-lu
E
DM-lu
LP-lu
Time (minute)
-60
-50
-40
-30
-20
-10
0
10
20
30
40
50
60
200
100
0
100
200
Position of Each Cell (μm)

Fig. 3

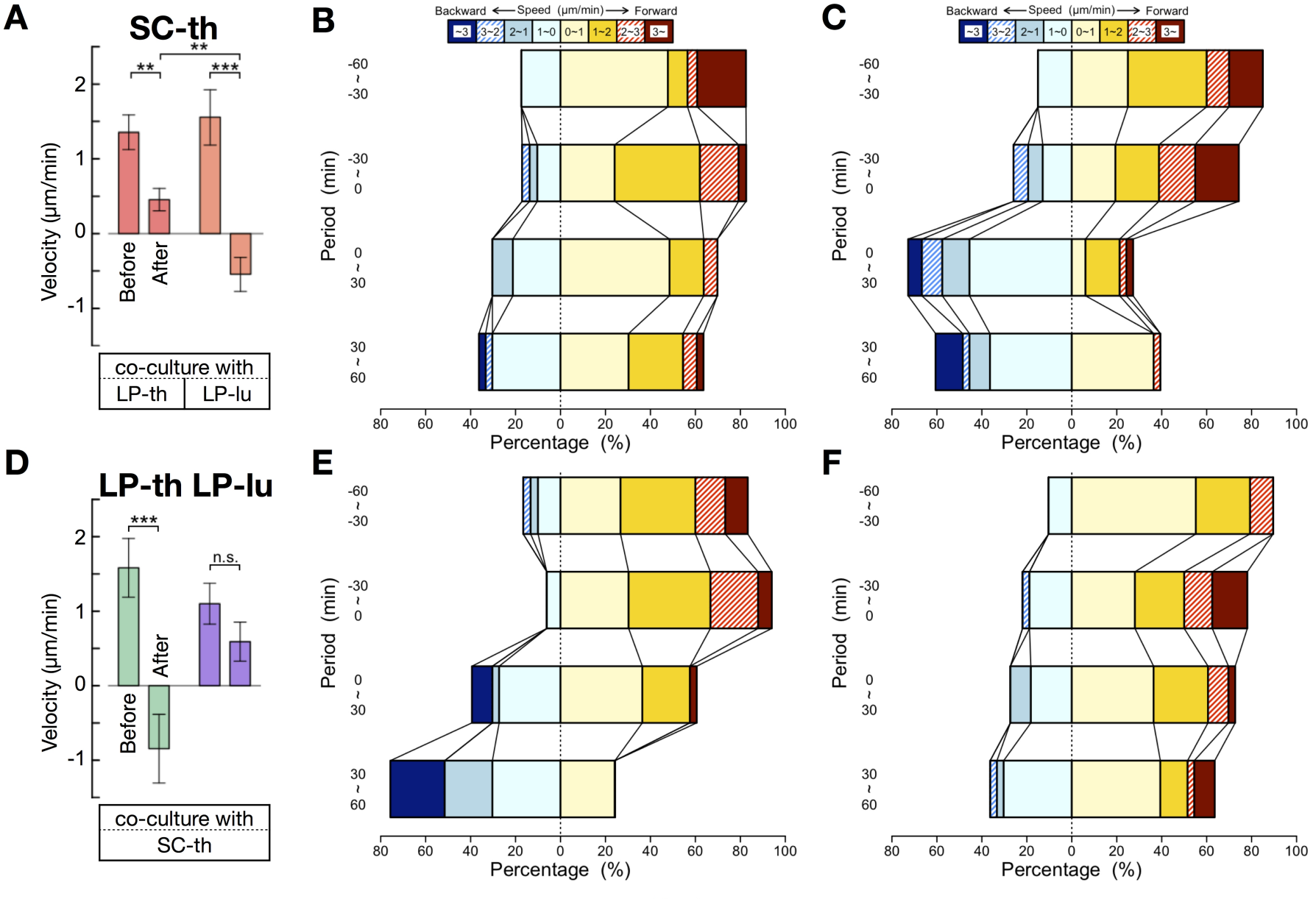
A
SC-th
Velocity (μm/min)
Before
After
co-culture with
LP-th
LP-lu
B
C
Backward ⟵ Speed (μm/min) ⟶ Forward
~3
3~2
2~1
1~0
0~1
1~2
2~3
3~
Period (min)
Percentage (%)
D
LP-th LP-lu
co-culture with
SC-th
n.s.
E
F

Fig. 4

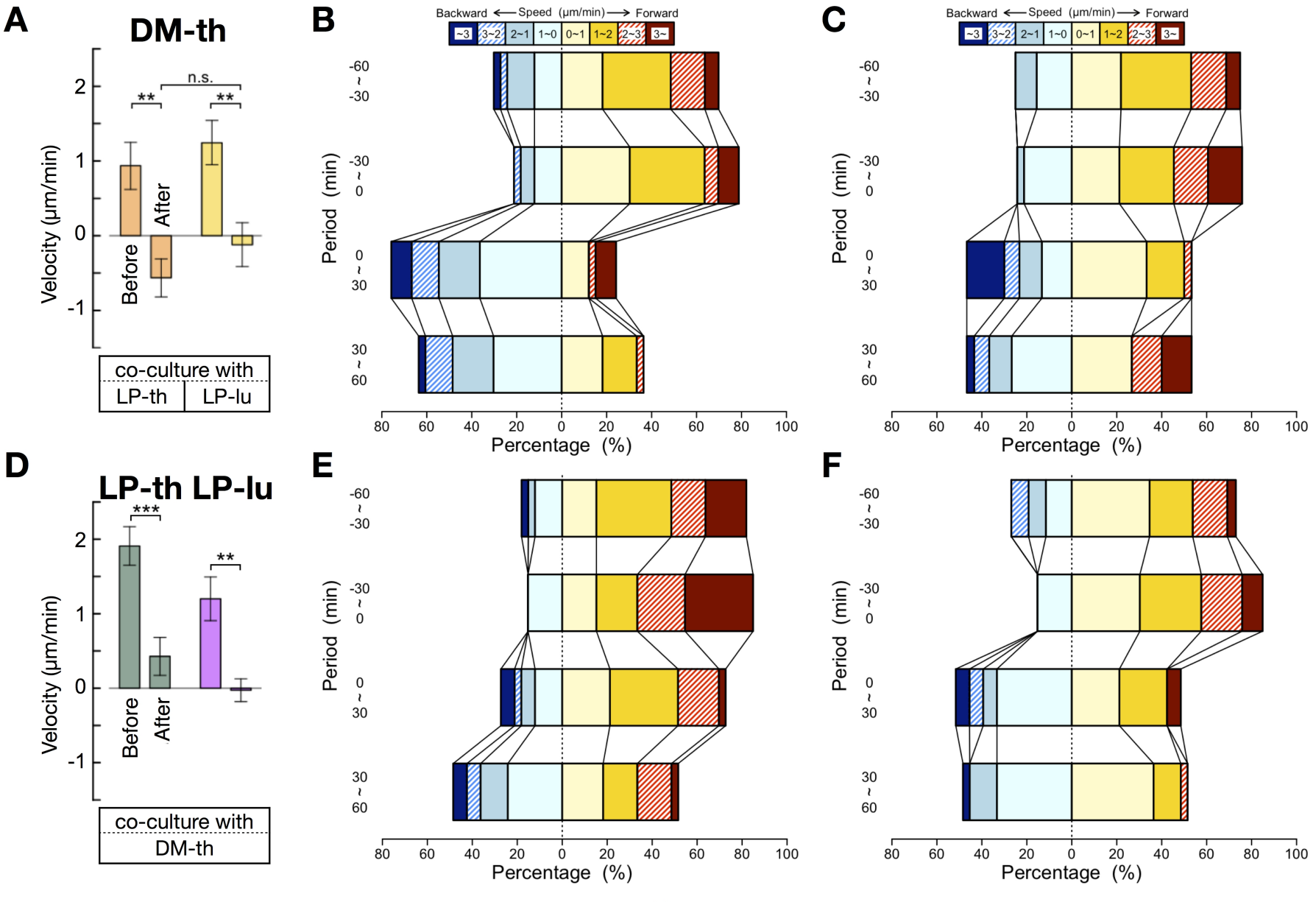
A
DM-th
Velocity (μm/min)
Before
After
n.s.
**
co-culture with
LP-th
LP-lu
B
C
Backward ← Speed (μm/min) → Forward
~3
3~2
2~1
1~0
0~1
1~2
2~3
3~
Period (min)
-60 ~ -30
-30 ~ 0
0 ~ 30
30 ~ 60
Percentage (%)
D
LP-th LP-lu
***
co-culture with
DM-th
E
F

Fig. 5

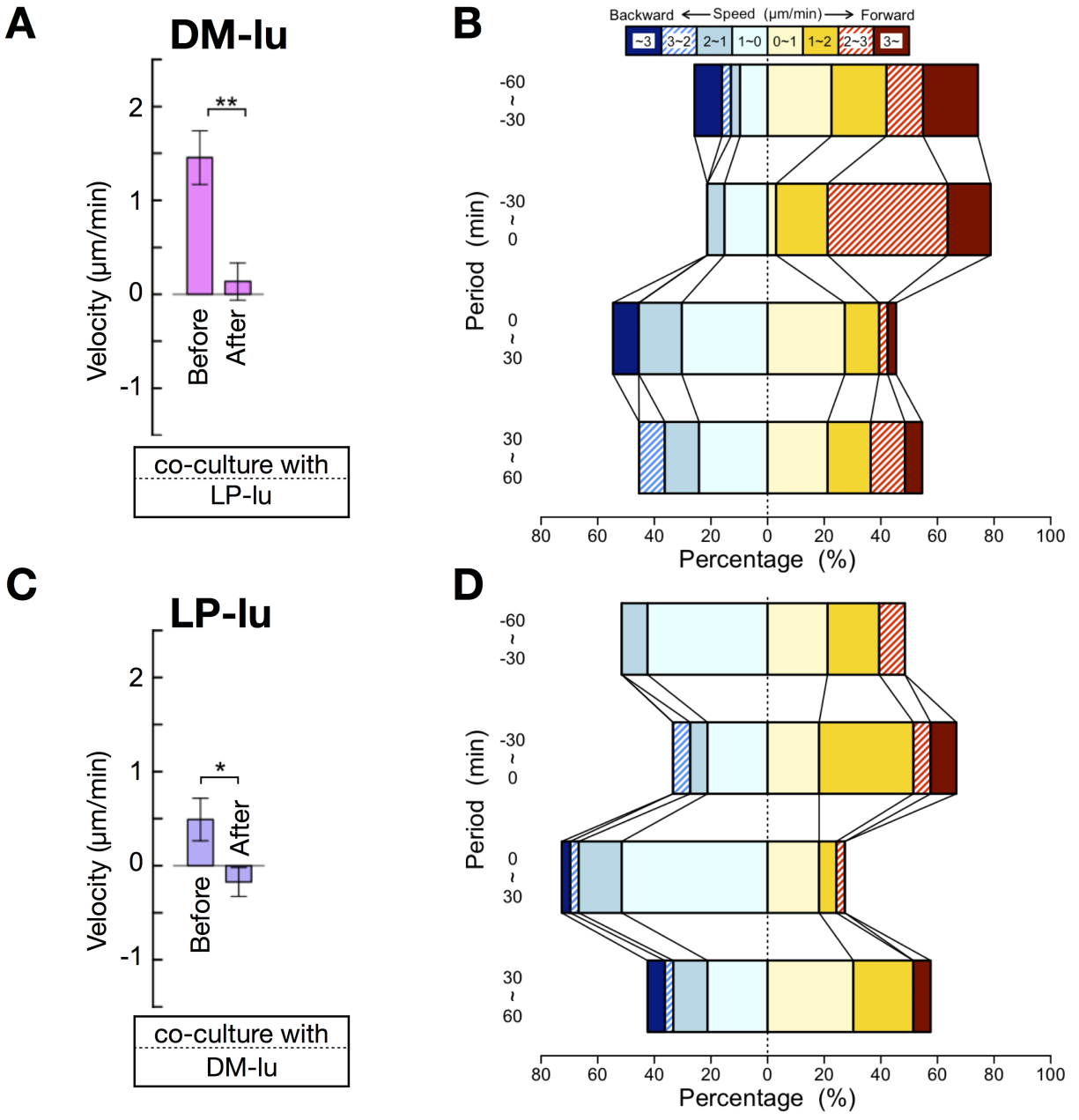
A
DM-lu
Velocity (μm/min)
2
1
0
-1
**
Before
After
co-culture with
LP-lu
B
Backward ⟵ Speed (μm/min) ⟶ Forward
~3
3~2
2~1
1~0
0~1
1~2
2~3
3~
Period (min)
-60 ~ -30
-30 ~ 0
0 ~ 30
30 ~ 60
80 60 40 20 0 20 40 60 80 100
Percentage (%)
C
LP-lu
Velocity (μm/min)
2
1
0
-1
*
Before
After
co-culture with
DM-lu
D
Period (min)
-60 ~ -30
-30 ~ 0
0 ~ 30
30 ~ 60
80 60 40 20 0 20 40 60 80 100
Percentage (%)

Fig. 6

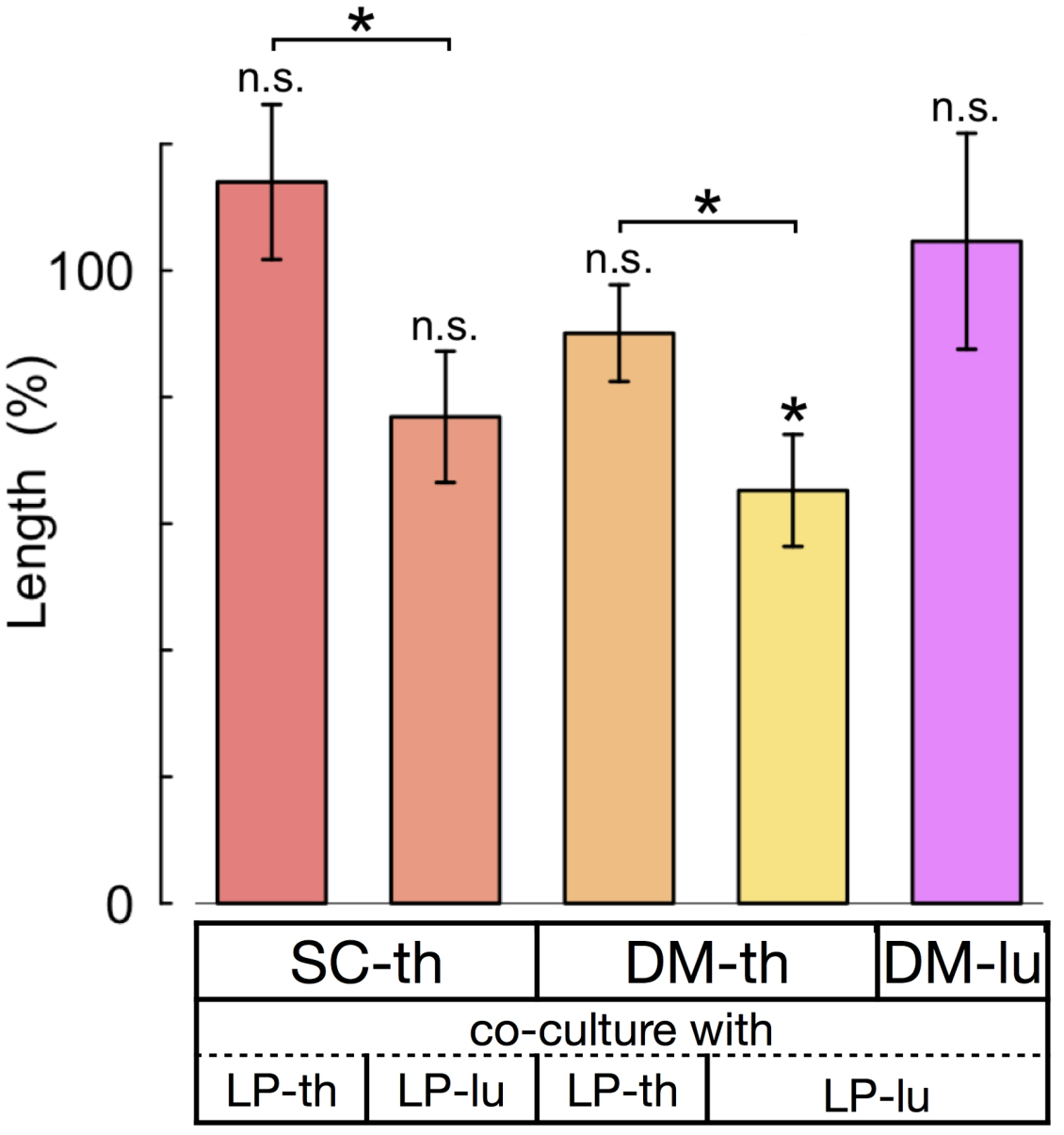
*
n.s.
n.s.
n.s.
*
n.s.
*
100
0
Length (%)
SC-th
DM-th
DM-lu
co-culture with
LP-th
LP-lu
LP-th
LP-lu

Fig. 7

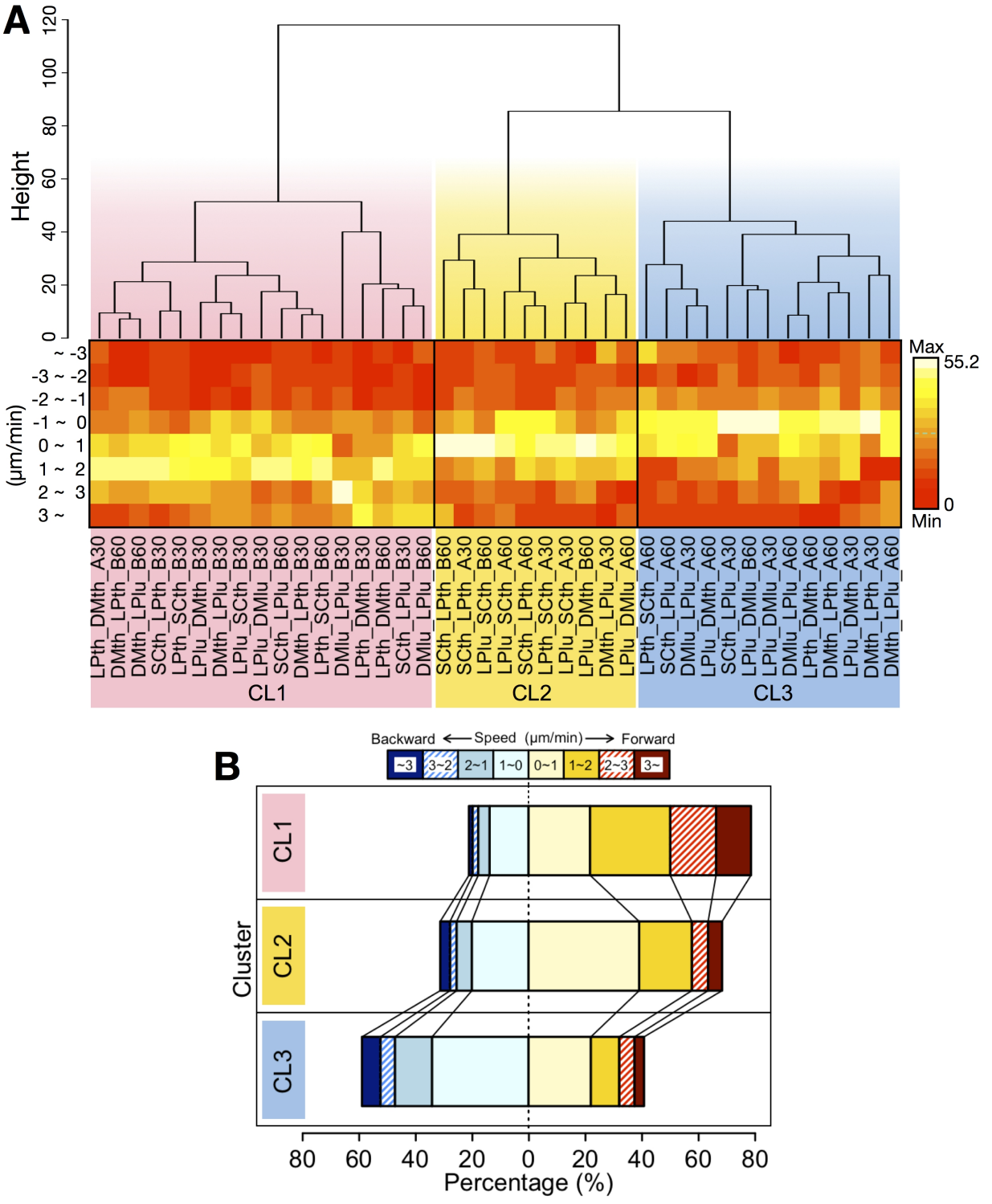

C

co-culture	SC-th vs. LP-th		SC-th vs. LP-lu		DM-th vs. LP-th		DM-th vs. LP-lu		DM-lu vs. LP-lu	
	SC-th	LP-th	SC-th	LP-lu	DM-th	LP-th	DM-th	LP-lu	DM-lu	LP-lu
Period (min) -60 ~ -30	CL2	CL1	CL1	CL2	CL1	CL1	CL1	CL2	CL1	CL3
-30 ~ 0	CL1	CL1	CL1	CL1	CL1	CL1	CL1	CL1	CL1	CL1
0 ~ 30	CL2	CL2	CL3	CL2	CL3	CL1	CL2	CL3	CL3	CL3
30 ~ 60	CL2	CL3	CL3	CL2	CL3	CL3	CL3	CL3	CL3	CL2

Fig. 8